

Surface ozone over the Tibetan Plateau controlled by stratospheric intrusion

Xiufeng Yin^{1,2}, Dipesh Rupakheti³, Guoshuai Zhang⁴, Jiali Luo⁵, Shichang Kang^{1,2}, Benjamin de Foy⁶,
Junhua Yang¹, Zhenming Ji⁷, Zhiyuan Cong⁸, Maheswar Rupakheti⁹, Ping Li^{2,10}, Yuling Hu^{10,*}, Qianggong
Zhang^{8,*}

¹ State Key Laboratory of Cryospheric Science, Northwest Institute of Eco-Environment and Resources, Chinese Academy of Science, Lanzhou 730000, China

² University of Chinese Academy of Sciences, Beijing 100049, China

³ Jiangsu Key Laboratory of Atmospheric Environment Monitoring and Pollution Control, Collaborative Innovation Center of Atmospheric Environment and Equipment Technology, School of Environmental Science and Engineering, Nanjing University of Information Science and Technology, Nanjing 210044, China

⁴ Chinese Academy of Environmental Planning, Beijing 100012, China

⁵ Key Laboratory for Semi-Arid Climate Change of the Ministry of Education, College of Atmospheric Sciences, Lanzhou University, Lanzhou 730000, China

⁶ Department of Earth and Atmospheric Sciences, Saint Louis University, St. Louis, MO, 63108, USA

⁷ School of Atmospheric Sciences, Key Laboratory for Climate Change and Natural Disaster Studies of Guangdong Province, Sun Yat-sen University, Guangzhou 510275, China

⁸ State Key Laboratory of Tibetan Plateau Earth System, Environment and Resources (TPESER), Institute of Tibetan Plateau Research, Chinese Academy of Sciences, Beijing 100101, China

⁹ Institute for Advanced Sustainability Studies, Potsdam, Germany

¹⁰ Key Laboratory of Land Surface Process and Climate Change in Cold and Arid Regions, Northwest Institute of Eco-Environment and Resources, Chinese Academy of Science, Lanzhou 730000, China

* *Correspondence to:* Qianggong Zhang (qianggong.zhang@itpcas.ac.cn) and Yuling Hu (huy1@lzb.ac.cn)

30 **Abstract:**

31 **Tibetan Plateau** is a global hotspot of stratospheric intrusion, and elevated surface ozone were observed at ground
32 monitoring sites. Still, links between the variability of surface ozone and stratospheric intrusion at regional scale remain unclear.
33 This study synthesized ground measurements of surface ozone over the **Tibetan Plateau** and analyzed their seasonal variations.
34 The monthly mean surface ozone concentrations **over the Tibetan Plateau** peaked earlier in the south in **April/May** and later in
35 the north in **June/July**. The migration of monthly surface ozone peaks was coupled with the synchronous movement of
36 tropopause fold and westerly jet that created a conducive conditions for stratospheric ozone intrusion. **Stratospheric ozone**
37 **intrusion significantly contributed to surface ozone across the Tibetan Plateau, especially for the areas with high surface ozone**
38 **concentrations during their peak-value month**. We demonstrated that monthly variation of surface ozone over the **Tibetan**
39 **Plateau** is mainly controlled by stratospheric intrusion, which warrants a proper consideration in understanding atmospheric
40 chemistry and impacts of ozone over this highland region and beyond.

41

42 **1. Introduction.**

43 **Tropospheric surface ozone (O₃)** has attracted great attention during the last decades due to its impact on the oxidative
44 capacity of the troposphere, the radiative forcing of the atmosphere, the detrimental effects on the vegetation and ecosystem,
45 and human health (Lu et al., 2018). The tropospheric (surface) ozone is controlled by in situ photochemical production in the
46 troposphere and by the intrusion of ozone-laden stratospheric air (Kumar et al., 2016; Yang et al., 2022). In contrast with other
47 air pollutants, tropospheric ozone is significantly influenced by stratospheric intrusion, especially at high elevation (Bracci et
48 al., 2012; Cristofanelli et al., 2010; Yin et al., 2017).

49 **Tibetan Plateau** is a vast plateau with an average elevation of ca. 4,500 m above sea level, making it the highest plateau
50 in the world. It is thus often referred to as “the roof of the world” or “the third pole” (Yao et al., 2012). With limited human
51 accessibility and low levels of industrialization, **Tibetan Plateau** is one of the most pristine regions in the world in terms of
52 most of the air pollutants (Yin et al., 2017) and is regarded as an ideal area for studying the atmospheric environment in the
53 free troposphere. It can provide deeper insights into changing background concentrations of atmospheric pollutants (Kang et
54 al., 2019). The **Tibetan Plateau** is recognized as a global hotspot of deep stratospheric intrusion, and elevated surface ozone
55 has been observed at some ground monitoring sites and very high concentrations of surface O₃ were reported (Cristofanelli et
56 al., 2010; Yin et al., 2017; Zhu et al., 2004). At sites, it was reported that vertical ozone flux from vertical transport by
57 convective and synoptic transport was prominent in the summer at Waliguan leading to high ozone levels (Ma et al., 2002; Ma
58 et al., 2005). Studies at Shangri-La and Nam Co in **Tibetan Plateau** indicated that the input of ozone from the stratosphere had
59 potential impacts on the seasonal variations of surface ozone at each site (Yin et al., 2017; Ma et al., 2014). Still, the link

60 between the variability of surface ozone and stratospheric intrusions at the regional scale remains unclear. In this study, 1)
61 ground observations of surface ozone at the sites over the Tibetan Plateau were used to reveal the difference of surface ozone
62 variation over the Tibetan Plateau from south to north. 2) WRF-Chem and CAM-chem simulations were used to identify the
63 impacts of long-range transport and in-situ photochemical production on surface ozone over the Tibetan Plateau. 3)
64 Distribution of tropopause fold frequencies (calculated by ERA-5 data), position of westerly jet (U component of winds) and
65 CAM-chem simulation was used to investigate the impact of stratospheric intrusion on surface ozone variation.

66 **2. Materials and Methods.**

67 **2.1. Surface measurements.**

68 This study synthesized ground measurements of surface ozone by analyzing the ground observation data collected at 13
69 sites (Shannan, Shigatse, Nyingchi, Lhasa, Changdu, Nagqu, Guoluozhou, Huangnanzhou, Hainanzhou, Haidongzhou, Xining,
70 Haibeizhou, and Haixizhou) ranging from the southern to the central and northeastern Tibetan Plateau (Figure 1 and Table S1
71 in Supplementary). Surface ozone concentrations during January 2016 to December 2021 at 13 sites were provided by the
72 China National Environmental Monitoring Center (<http://106.37.208.233:20035/>). Surface ozone was measured with the UV-
73 spectrophotometry method. The specifications and test procedures of ozone followed the Specifications and Test Procedures
74 for Ambient Air Quality Continuous Automated Monitoring System for ozone (National Environmental Protection Standards
75 of the People's Republic of China, HJ 654-2013). The inlet of the instrument was 3-20 m above the ground surface, 1 m higher
76 than the roof of the building or the wall. The observation stations were located at least 50 m from any obvious stationary
77 pollution sources. The data quality assurance and controls followed technical guidelines on environmental monitoring quality
78 management (National Environmental Protection Standards of the People's Republic of China, HJ 630-2011), and the data
79 were checked for validity based on ambient air quality standards (National Standards of the People's Republic of China, GB
80 3095-2012).

81 **2.2. Reanalysis data.**

82 The ECMWF (European Centre for Medium-Range Weather Forecasts) ERA-5 data (0.28125° latitude × 0.28125°
83 longitude horizontal resolution, and 137 vertical levels) (Hoffmann et al., 2019) were used to analyze the monthly mean
84 meridional cross-section structures of troposphere and stratosphere over the Tibetan Plateau. Monthly mean total tropopause
85 fold frequency was investigated in this study and tropopause fold was defined by 2 pvu (potential vorticity unit) iso-surface
86 and identified by the method described in Luo et al. (2019). Tropopause folds were defined as multiple crossings of the
87 dynamical tropopause in a vertical profile.

88 **2.3. Model simulation.**

89 The Community Atmosphere Model with Chemistry (CAM-chem), a global model, was used for simulations of global

90 tropospheric and stratospheric atmospheric composition (Lamarque et al., 2012) provided by University Corporation for
91 Atmospheric Research (<https://www.acom.ucar.edu/cam-chem/cam-chem.shtml>). The horizontal resolution for CAM-chem is
92 $0.5^\circ \times 0.5^\circ$. CAM-chem uses the MOZART (Model for OZone And Related chemical Tracers) chemical mechanisms
93 (Lamarque et al., 2012), with various choices of complexity for tropospheric and stratospheric chemistry. The O_{3S} variable, a
94 stratospheric ozone tracer that represents the amount of ozone in the troposphere originated in the stratosphere, in CAM-chem
95 simulation was used in this study to indicate the intensity of the ozone transported from the stratosphere (Tilmes et al., 2016).
96 O_{3S}/O_3 ratio was calculated to investigate the intensity of impacts from the stratospheric intrusion to ozone concentration in
97 troposphere.

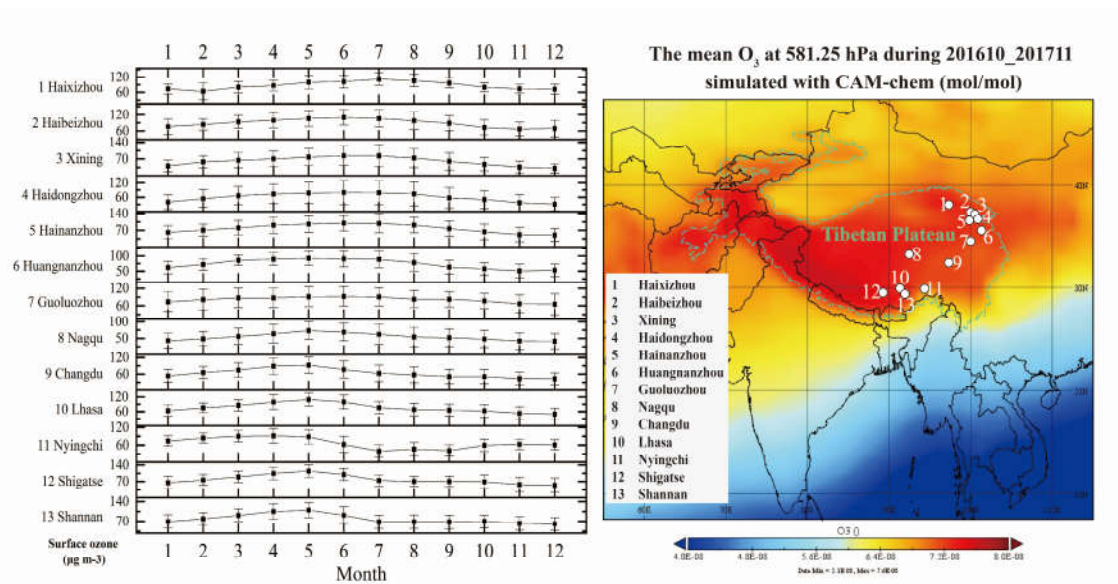
98 Weather Research and Forecasting model coupled with Chemistry (WRF-Chem) was conducted by the setup adopted in
99 Yang et al. (2022) to investigate the long-range transport from South Asia and local photochemical generation of ozone over
100 the Tibetan Plateau. The model domain has 25-km grid spacing and covers South Asia and the TP, with 155 and 135 grid cells
101 in the west–east and north–south directions, respectively. The vertical configuration of the model includes 35 vertical sigma
102 layers at the top pressure of 50 hPa. National Centers for Environmental Prediction Final (NCEP FNL) analysis data with a
103 horizontal resolution of $1^\circ \times 1^\circ$ at 6-h time intervals is used for the meteorological initial and boundary conditions. Both CAM-
104 chem and WRF-Chem simulations were conducted for an entire year, from 1 November 2016 to 30 November 2017. The first
105 month was considered the model spin-up time and was not analyzed. In WRF-Chem simulation, experiments with 2 setups
106 were conducted as setup 1 (CO and NO₂ in South Asia were set to 0 to investigate the influence of long-range transport from
107 South Asia) and setup 2 (CO and NO₂ in the Tibetan Plateau were set to 0 to investigate the influence of local photochemical
108 generation of ozone over the Tibetan Plateau).

109 **3. Results and Discussion.**

110 **3.1. Surface ozone variations over the Tibetan Plateau.**

111 The mean surface ozone concentrations during 2016-2021 at 13 sites over Tibetan Plateau peaked in different months and
112 moved gradually from April/May in the south to June/July in the north (Figure 1). A similar result was obtained in the month-
113 to-month variation of mean ozone concentrations at 13 sites (Figure S1 in Supplementary). It is noteworthy that such regular
114 migration of monthly ozone peaks occurred at large geographical scale, and surface ozone concentrations peaked
115 synchronously at sites in the same zone despite the differences in size of cities and baseline levels of surface ozone. Previous
116 studies also found that the sites in adjacent areas showed similar monthly variation of surface ozone (Ma et al., 2014; Lin et
117 al., 2015; Ran et al., 2014; Cristofanelli et al., 2010; Zhu et al., 2004; Yin et al., 2017). The occurrence of the highest monthly
118 concentrations of surface ozone is different in different areas over the Tibetan Plateau, ranging from April to July.

119



120
 121 Figure 1. Study sites (right) and their monthly mean surface ozone variations during January 2016 to December 2021
 122 across the Tibetan Plateau (left) used in this study. Map of yearly mean concentration of surface ozone during January 2016
 123 to December 2021 at 581.25 hPa simulated with CAM-chem is shown with colored shadings.

124
 125 **3.2. Long-range transport and photochemical production are not likely the dominator of surface ozone.**

126 We compared the simulated surface temperature (T2), relative humidity (RH2), wind at 10 meters (wind10), and wind at
 127 500 hPa, with surface observations provided by China Meteorological Data Service Centre (<http://data.cma.cn/>) and ERA
 128 interim reanalysis datasets provided by ECMWF (<https://apps.ecmwf.int/datasets/>). It was found that simulation configuration
 129 captured the meteorological fields well, which is crucial to assure prediction accuracy of air pollutant concentrations (Figure
 130 S2-S5). Besides, surface ozone concentrations from ground observations, WRF-Chem, and CAM-chem were compared and
 131 showed a good fit (Figure S6).

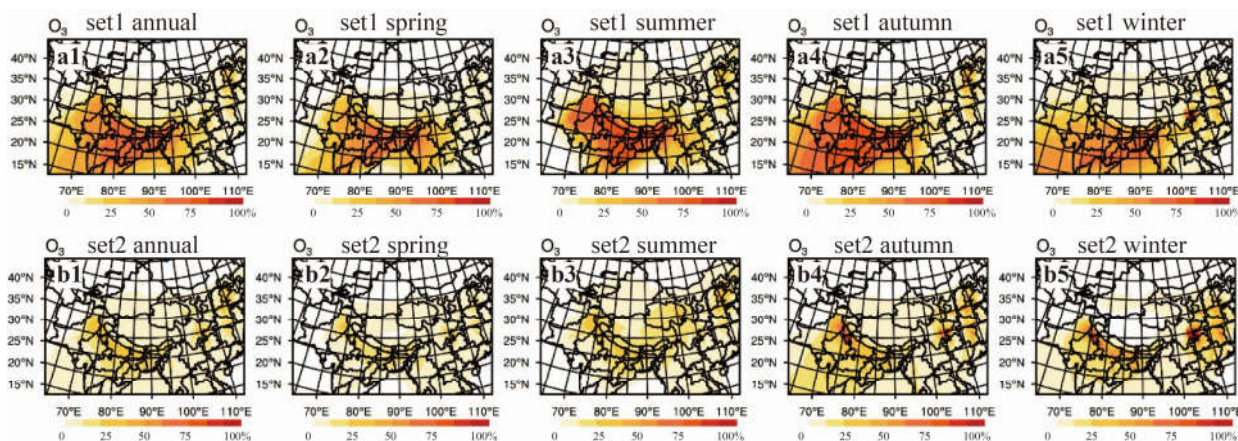
132 Generally, elevated tropospheric ozone budgets at ground sites result from three processes: in-situ photochemical
 133 production, long-range transport, and influx of ozone from the stratosphere. South Asia is one of the biggest sources of air
 134 mass that arrived the Tibetan Plateau by long-range transport (Yin et al., 2021) and the concentrations of air pollutions,
 135 including the precursors of surface ozone (e.g. CO, VOCs), in South Asia were high (Kumar et al., 2018). Indicated by results
 136 in WRF-Chem simulation setup 1 (Figure 2a), long-range transport from South Asia contributed to the surface ozone in the
 137 Tibetan Plateau from 9.45% to 20.28% in each season with annual average in 14.13% (Table 1), showing a limited impact.

138
 139 Table 1. The influence ratios of long-range transport (WRF-Chem set 1) and in-situ photochemical production (WRF-Chem
 140 set 2) on surface ozone over the Tibetan Plateau.

	Annual	Spring	Summer	Autumn	Winter
--	--------	--------	--------	--------	--------

WRF-Chem set 1	14.13%	13.18%	20.28%	14.52%	9.45%
WRF-Chem set 2	10.46%	8.43%	17.44%	11.95%	5.24%

141



142

143

144

Figure 2. The influence ratios of long-range transport (WRF-Chem set 1) and in-situ photochemical production (WRF-Chem set 2) on surface ozone over the Tibetan Plateau.

145

146

147

148

149

150

151

152

153

154

The local photochemical production of ozone is generated through a chain of photochemical oxidation of CO and VOCs (volatile organic compounds). The monthly variation in surface ozone at three different types of sites in the central Tibetan Plateau (Lhasa: urban site; Dangxiang: rural site; Nam Co: remote site) with varying conditions of ozone precursors were similar (Yin et al., 2017), implying the limited impact from local photochemical production of ozone on the monthly variation of surface ozone at these sites. Indicated by results in WRF-Chem simulation setup 2 (Figure 2b), local photochemical generation of ozone over the Tibetan Plateau contributed to the surface ozone in the Tibetan Plateau from 5.24% to 17.44% in each season with annual average in 10.46% (Table 1). Furthermore, the net ozone photochemical production was found to be negative in the summer when surface ozone reached a maximum in the northeastern Tibetan Plateau (Zhu et al., 2004; Ma et al., 2002). Therefore, the monthly mean surface ozone peaks in Tibetan Plateau were not mainly attributed to the local photochemical production of ozone.

155

156

157

158

159

Even in the summer, when the contributions from these two factors are high, the total contribution from both long-range transport from South Asia and local photochemical generation of ozone over the Tibetan Plateau to the variation of surface ozone on the Tibetan Plateau was less than 38% (total contribution = 37.72%). Based on the above results, we can infer that the variation of surface ozone over the Tibetan Plateau is dominated by other factors than long-range transport and in-situ photochemical production.

160

3.3. Evidences from reanalysis data and simulation for stratospheric intrusion.

161

162

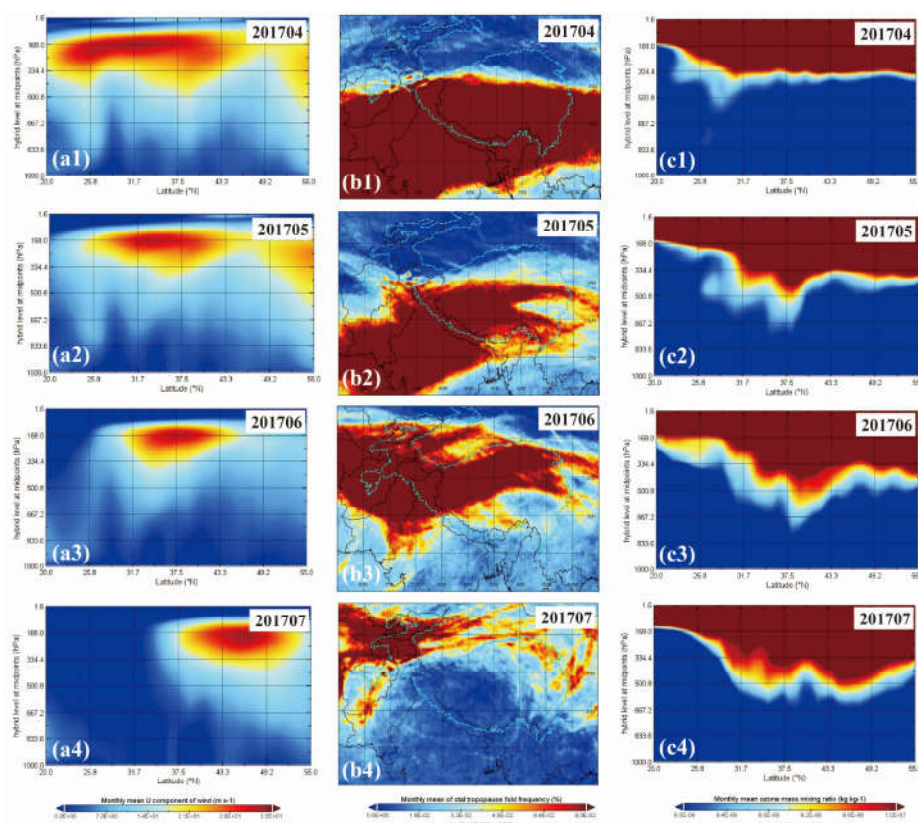
163

Rather than long-range transport and photochemical production, the stratospheric influx of ozone is likely a main contributor to the surface ozone over the Tibetan Plateau. The impact of stratospheric intrusion on the surface ozone can be supported by the monthly averages of the total tropopause fold frequencies (tropopause fold was indicated by 2 potential

164 vorticity unit iso-surface, in Luo et al., (2019)) over the Tibetan Plateau (Figure 3). It was found that the displacement of the
 165 tropopause fold in the Tibetan Plateau was controlled by the movement of the westerly jet (Luo et al., 2019). The monthly
 166 mean meridional cross-section of westerly jet (indicated by the maximum speed of the U component of winds), tropopause
 167 fold frequencies, and the transport of ozone from the stratosphere to the troposphere was calculated and visualized from April
 168 to July 2017 (Figure 3).

169 In April, the westerly jet was mainly above the region within 25°N-40°N (Figure 3). The highest frequencies of total
 170 tropopause fold were mainly distributed in ca. 25-35°N latitude band covering parts of South Asia, the southern and the central
 171 Tibetan Plateau (Figure 3). The most hotspot of stratospheric ozone intrusion to troposphere was in ~29°N (Figure 3), similar
 172 with the area with high ozone concentration in April (Figure 4). In May, the westerly jet was northward moved to be center
 173 with ~35°N. The stratospheric ozone intrusion to troposphere was strong in ~37.5°N and ~30°N similar with the areas with
 174 high frequencies of total tropopause fold (Figure 3), contributing to high ozone concentrations in these areas (Figure 3). In
 175 June, the westerly jet was moved northward and hotspot of stratospheric ozone intrusion to troposphere was in ~38°N and
 176 ~32°N (Figure 3) and these two areas were in high ozone concentrations (Figure 4). In July, the westerly jet was even more
 177 northward moved and only the northeastern Tibetan Plateau was under significant impact of stratospheric ozone intrusion
 178 within 31.7°N-40°N (Figure 3) and induced high ozone concentration in the northeastern Tibetan Plateau (Figure 4). Consistent
 179 with the monthly spatial distribution of the westerly jet and tropopause fold occurrence, stratospheric ozone intrusion showed
 180 a northward movement from April to July.

181



182

183 Figure 3. Monthly mean meridional cross-section of ERA-5 data at 91°E (~ the central Tibetan Plateau) showing the
184 zonal winds c) and ozone (d) in April, May, June, and July in 2017. Monthly average of total tropopause fold frequencies (b)
185 in April, May, June, and July in 2017.

186

187 **3.4. Impact of stratospheric intrusion evidenced by stratospheric ozone tracer.**

188 In the southern Tibetan Plateau, it was stated that the surface ozone mixing ratios were significantly increased by the
189 stratospheric intrusions (+13 ppb during stratospheric intrusions) (Cristofanelli et al., 2010). The previous studies stated that
190 the peak of surface ozone in June at Waliguan in the northeastern Tibetan Plateau was due to the downward transport of ozone
191 from the upper troposphere and lower stratosphere (Ma et al., 2005; Ding and Wang, 2006). This is evidenced by analysis of a
192 stratospheric ozone tracer of O_{3s} (a stratospheric ozone tracer that represents the amount of ozone in the troposphere originated
193 in the stratosphere in CAM-chem) across the south-north transection of the Tibetan Plateau. Figure 4 (a1-a4) showed the
194 surface ozone variation from April 2017 to July 2017 over the Tibetan Plateau in CAM-chem simulation. In April 2017, the
195 hotspot area of high ozone concentration mainly distributed in the southern Tibetan Plateau which was consistent with the
196 distribution of high O_{3s} concentration (Figure 4a). The average of O_{3s}/O_3 representing indicator of the stratospheric ozone
197 contribution, demonstrated that 36.5% of surface ozone in the hotspot of the southern Tibetan Plateau (85°E-92.5°E and
198 27.8°N-30.6°N) was contributed by stratospheric ozone. In May and June 2017, the southern Tibetan Plateau was still in high
199 ozone concentration and part of the northeastern Tibetan Plateau became a new hotspot with high ozone concentration and O_{3s}
200 in the northeastern Tibetan Plateau was in high concentration (Figure 4b). The average of O_{3s}/O_3 was 35.9% in May and 29.5%
201 in June in the northeastern Tibetan Plateau (the region within 90°E-100°E and 34.4°N-39.1°N). The average of O_{3s}/O_3 was
202 higher than 25% in the southern Tibetan Plateau (85°E-90°E and 27.8°N-30.6°N) in May and in the southwestern Tibetan
203 Plateau (80°E-85°E and 27.8°N-32.5°N). In July 2017, only the northeastern Tibetan Plateau was in high ozone concentration
204 and O_{3s}/O_3 was higher than 25% in this region. It can be stated that stratospheric ozone intrusion could elevate at least 25% of
205 surface ozone over the Tibetan Plateau at hotspot regions during April to July.

206

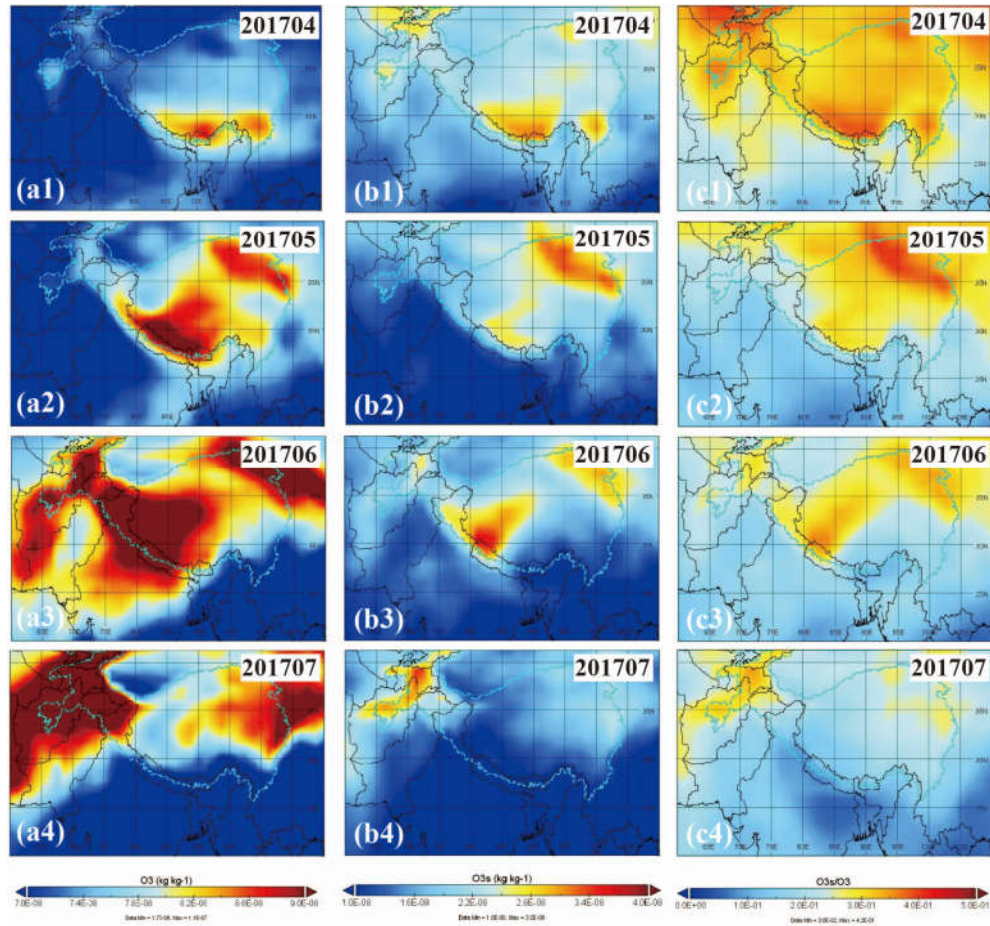


Figure 4. Monthly average of (a) ozone, (b) O_{3s}, and (c) O_{3s}/O₃ at 581.25 hPa in April, May, June, and July in 2017.

The location of the Tibetan Plateau is shown with cyan contour in the maps.

4. Conclusions.

The ground measurements of surface ozone at 13 sites spread across the Tibetan Plateau were used for the first time in this study, as opposed to previous studies which focused mostly on individual sites. Simulation results from WRF-Chem, CAM-chem and analysis of ERA-5 reanalysis data were used to investigate the influences of long-range transport and in-situ photochemical production, and downward influx of ozone from the stratosphere on the variation in surface ozone. Results showed that the peak of monthly mean surface ozone concentration occurs first over the southern and the central Tibetan Plateau in April/May, and then moves progressively northwards in June/July. Such peak shift is concurrent with northward movement of the tropopause folds and westerly jet, which act as the two main control mechanisms. The position of tropopause folds was controlled by the position of the westerly jet and created the conditions conducive for the influx of ozone rich air from the deep stratosphere to the troposphere. The migration of the folds led to a similar migration from south to north of stratospheric intrusions. This lead to a significant contribution of stratospheric intrusions to the surface ozone, elevating the surface ozone concentrations. Long-range transport and in-situ photochemical production of ozone can lead to limited variation

223 of surface ozone over the Tibetan Plateau. We suggest that the transport of stratospheric ozone to the surface is a regionally
224 coherent important contributor to surface ozone across the Tibetan Plateau, which needs a proper consideration in
225 understanding the atmospheric chemistry and the impacts of ozone over this highland region and beyond.

226

227 **Acknowledgments:** This study was supported by the Second Tibetan Plateau Scientific Expedition and Research Program
228 (STEP), Grant No. 2019QZKK0605, the National Natural Science Foundation of China (41907328), and State Key Laboratory
229 of Cryospheric Science (SKLCS-ZZ-2022). X.F. Yin acknowledges financial support from the Chinese Academy of Sciences
230 "Light of West China" Program. Q. G. Zhang acknowledges financial support from the Youth Innovation Promotion
231 Association of CAS (202022). We acknowledge the China National Environmental Monitoring Center, the European Centre
232 for Medium-Range Weather Forecasts, the Institute of Atmospheric Sciences and Climate, University Corporation for
233 Atmospheric Research, and the National Bureau of Statistics of China for providing the data.

234

235 **Data Availability Statement:** Surface ozone data at 13 sites are available through the China National Environmental
236 Monitoring Center (<http://106.37.208.233:20035/>). ERA-5 data are available through the European Centre for Medium-Range
237 Weather Forecasts (<https://cds.climate.copernicus.eu/cdsapp#!/dataset/reanalysis-era5-single-levels?tab=form>, after login).
238 CAM-chem data are available through University Corporation for Atmospheric Research (<https://www.acom.ucar.edu/cam-chem/cam-chem.shtml>).

240

241 **Author contributions:** Xiufeng Yin: Conceptualization, visualization, writing - original draft. Benjamin de Foy, Dipesh
242 Rupakheti, Zhenming Ji, Zhiyuan Cong, Guoshuai Zhang, and Maheswar Rupakheti: Writing - review & editing.
243 Junhua Yang and Ping Li: Visualization. Yuling Hu and Jiali Luo: Visualization, writing – review. Shichang Kang and
244 Qiangong Zhang: Conceptualization, writing - review & editing.

245 **Competing interests**

246 The authors declare no competing interests.

247

248 **References**

249 Bracci, A., Cristofanelli, P., Sprenger, M., Bonafè, U., Calzolari, F., Duchi, R., Laj, P., Marinoni, A., Roccatò, F., and
250 Vuillermoz, E.: Transport of Stratospheric Air Masses to the Nepal Climate Observatory–Pyramid (Himalaya; 5079 m
251 MSL): A Synoptic-Scale Investigation, *Journal of applied meteorology and climatology*, 51, 1489-1507, 2012.

252 Cristofanelli, P., Bracci, A., Sprenger, M., Marinoni, A., Bonafè, U., Calzolari, F., Duchi, R., Laj, P., Pichon, J. M., Roccatò,
253 F., Venzac, H., Vuillermoz, E., and Bonasoni, P.: Tropospheric ozone variations at the Nepal Climate Observatory-
254 Pyramid (Himalayas, 5079 m a.s.l.) and influence of deep stratospheric intrusion events, *Atmospheric Chemistry and*
255 *Physics*, 10, 6537-6549, 10.5194/acp-10-6537-2010, 2010.

256 Hoffmann, L., Günther, G., Li, D., Stein, O., Wu, X., Griessbach, S., Heng, Y., Konopka, P., Müller, R., and Vogel, B.: From
257 ERA-Interim to ERA5: the considerable impact of ECMWF's next-generation reanalysis on Lagrangian transport
258 simulations, *Atmospheric Chemistry and Physics*, 19, 3097-3124, 2019.

259 Kang, S., Zhang, Q., Qian, Y., Ji, Z., Li, C., Cong, Z., Zhang, Y., Guo, J., Du, W., and Huang, J.: Linking atmospheric pollution
260 to cryospheric change in the Third Pole region: current progress and future prospects, *National Science Review*, 6, 796-
261 809, 2019.

262 Kumar, R., Barth, M. C., Pfister, G., Delle Monache, L., Lamarque, J., Archer-Nicholls, S., Tilmes, S., Ghude, S., Wiedinmyer,
263 C., and Naja, M.: How will air quality change in South Asia by 2050?, *Journal of Geophysical Research: Atmospheres*,
264 123, 1840-1864, 2018.

265 Kumar, V., Sarkar, C., and Sinha, V.: Influence of post-harvest crop residue fires on surface ozone mixing ratios in the NW
266 IGP analyzed using 2 years of continuous in situ trace gas measurements, *Journal of Geophysical Research: Atmospheres*,
267 121, 3619-3633, 2016.

268 Lamarque, J. F., Emmons, L. K., Hess, P. G., Kinnison, D. E., Tilmes, S., Vitt, F., Heald, C. L., Holland, E. A., Lauritzen, P.
269 H., Neu, J., Orlando, J. J., Rasch, P. J., and Tyndall, G. K.: CAM-chem: description and evaluation of interactive
270 atmospheric chemistry in the Community Earth System Model, *Geosci. Model Dev.*, 5, 369-411, 10.5194/gmd-5-369-
271 2012, 2012.

272 Lin, W., Xu, X., Zheng, X., Dawa, J., Baima, C., and Ma, J.: Two-year measurements of surface ozone at Dangxiong, a remote
273 highland site in the Tibetan Plateau, *Journal of Environmental Sciences*, 31, 133-145, 2015.

274 Lu, X., Hong, J., Zhang, L., Cooper, O. R., Schultz, M. G., Xu, X., Wang, T., Gao, M., Zhao, Y., and Zhang, Y.: Severe surface
275 ozone pollution in China: a global perspective, *Environmental Science & Technology Letters*, 5, 487-494, 2018.

276 Luo, J., Liang, W., Xu, P., Xue, H., Zhang, M., Shang, L., and Tian, H.: Seasonal Features and a Case Study of Tropopause
277 Folds over the Tibetan Plateau, *Advances in Meteorology*, 2019, 2019.

278 Ma, J., Liu, H., and Hauglustaine, D.: Summertime tropospheric ozone over China simulated with a regional chemical transport
279 model 1. Model description and evaluation, *Journal of Geophysical Research: Atmospheres*, 107, ACH 27-21-ACH 27-
280 13, 2002.

281 Ma, J., Zheng, X., and Xu, X.: Comment on “Why does surface ozone peak in summertime at Waliguan?” by Bin Zhu et al,
282 *Geophysical research letters*, 32, 2005.

283 Ma, J., Lin, W. L., Zheng, X. D., Xu, X. B., Li, Z., and Yang, L. L.: Influence of air mass downward transport on the variability
284 of surface ozone at Xianggelila Regional Atmosphere Background Station, southwest China, *Atmospheric Chemistry and*
285 *Physics*, 14, 5311-5325, 10.5194/acp-14-5311-2014, 2014.

286 Putero, D., Landi, T. C., Cristofanelli, P., Marinoni, A., Laj, P., Duchi, R., Calzolari, F., Verza, G. P., and Bonasoni, P.:
287 Influence of open vegetation fires on black carbon and ozone variability in the southern Himalayas (NCO-P, 5079 m
288 a.s.l.), *Environ Pollut*, 184, 597-604, 10.1016/j.envpol.2013.09.035, 2014.

289 Ran, L., Lin, W. L., Deji, Y. Z., La, B., Tsering, P. M., Xu, X. B., and Wang, W.: Surface gas pollutants in Lhasa, a highland
290 city of Tibet - current levels and pollution implications, *Atmospheric Chemistry and Physics*, 14, 10721-10730,
291 10.5194/acp-14-10721-2014, 2014.

292 Tilmes, S., Lamarque, J. F., Emmons, L. K., Kinnison, D. E., Marsh, D., Garcia, R. R., Smith, A. K., Neely, R. R., Conley, A.,
293 Vitt, F., Val Martin, M., Tanimoto, H., Simpson, I., Blake, D. R., and Blake, N.: Representation of the Community Earth
294 System Model (CESM1) CAM4-chem within the Chemistry-Climate Model Initiative (CCMI), *Geosci. Model Dev.*, 9,
295 1853-1890, 10.5194/gmd-9-1853-2016, 2016.

296 Xu, X., Lin, W., Xu, W., Jin, J., Wang, Y., Zhang, G., Zhang, X., Ma, Z., Dong, Y., and Ma, Q.: Long-term changes of regional
297 ozone in China: implications for human health and ecosystem impacts, *Elem Sci Anth*, 8, 2020.

298 Yang, J., Wang, K., Lin, M., Yin, X., and Kang, S.: Not biomass burning but stratospheric intrusion dominating tropospheric

299 ozone over the Tibetan Plateau, *Proceedings of the National Academy of Sciences*, 119, e2211002119, 2022.

300 Yao, T., Thompson, L., Yang, W., Yu, W., Gao, Y., Guo, X., Yang, X., Duan, K., Zhao, H., and Xu, B.: Different glacier
301 status with atmospheric circulations in Tibetan Plateau and surroundings, *Nature Climate Change*, 2, 663-667, 2012.

302 Yin, X., Kang, S., de Foy, B., Cong, Z., Luo, J., Zhang, L., Ma, Y., Zhang, G., Rupakheti, D., and Zhang, Q.: Surface ozone
303 at Nam Co in the inland Tibetan Plateau: variation, synthesis comparison and regional representativeness, *Atmospheric
304 Chemistry and Physics*, 17, 11293-11311, 10.5194/acp-17-11293-2017, 2017.

305 Yin, X., Kang, S., Foy, B. d., Rupakheti, D., Rupakheti, M., Cong, Z., Wan, X., Zhang, G., and Zhang, Q.: Impacts of Indian
306 summer monsoon and stratospheric intrusion on air pollutants in the inland Tibetan Plateau, *Geoscience Frontiers*, 12,
307 101255, <https://doi.org/10.1016/j.gsf.2021.101255>, 2021.

308 Zhu, B., Akimoto, H., Wang, Z., Sudo, K., Tang, J., and Uno, I.: Why does surface ozone peak in summertime at Waliguan?,
309 *Geophysical research letters*, 31, 2004.

310

311